Available online at www.sciencedirect.com
SCIENCE DIRECT
Polymer 47 (2006) 3315–3324
polymer
www.elsevier.com/locate/polymer

Suspension polymerization of thermally expandable core/shell particles

Magnus Jonsson [a], Ove Nordin [b], Eva Malmström [a,*], Claes Hammer [b]

[a] *Department of Fibre and Polymer Technology, School of Chemical Science and Engineering, KTH, Royal Institute of Technology, SE-100 44 Stockholm, Sweden*
[b] *Akzo Nobel, Box 13000, SE-850 13 Sundsvall, Sweden*

Received 14 November 2005; received in revised form 16 February 2006; accepted 5 March 2006
Available online 3 April 2006

Abstract

Acrylonitrile (AN)-methacrylonitrile (MAN) copolymer particles with a core/shell structure were prepared by suspension polymerization. The particles were about 10–20 μm in diameter and had a hollow core containing an inert hydrocarbon. The influence of the monomer feed ratio and the polymerization temperature on the particle morphology was studied. One purpose of this study was to determine the boundaries for achieving a core/shell structure with the polymer encapsulating the hydrocarbon. When polymerizing at 62 °C, it was found that an initial AN/MAN feed ratio (f_{AN}) between 0.15 and 0.9 results in core/shell particles with encapsulated hydrocarbon. f_{AN} lower than 0.15 yielded solid particles with no hydrocarbon encapsulated while f_{AN} higher than 0.9 yielded particles built up entirely from agglomerates of smaller primary particles. In contrast, when polymerizing at 80 °C, a much narrower span of f_{AN} (0.5–0.85) yielded particles with hydrocarbon encapsulated. The influence on monomer conversion and the molecular weight of the polymer was also studied.

Keywords: Suspension polymerization; Core/shell morphology; Encapsulation

1. Introduction

Thermally expandable microspheres are polymeric particles widely used in industry as blowing agents or as light weight fillers. They are 5–50 μm sized particles in which a thermoplastic acrylonitrile copolymer encapsulates an inert low boiling hydrocarbon. Upon heating, the particles expand, reducing the density from 1100 kg/m^3 to approximately 20–30 kg/m^3. Expansion occurs as the thermoplastic shell softens (T_g), while the encapsulated hydrocarbon gasifies, increasing the internal pressure in the particle.

Thermally expandable microspheres have proven to be a very useful product in a wide variety of applications. In printing inks as they enable the production of surface textures on wallpaper and textile [1]. They are also excellent weight-reducing additives as a 3% (by weight) addition of microspheres can reduce the weight of various matrices by as much as 40% [2]. Apart from solely reducing the weight, they sometimes also improve the physical properties of the resulting product [3].

This kind of thermally expandable particle was originally invented by Dow Chemical Co. [1], and has been further developed by others [4–6]. The dominating manufacturing technique [1,4,5], and the one used in this study, is based on a free-radical suspension polymerization [7–9] of vinyl type monomers with an in situ encapsulation of the blowing agent. In this process, a monomer phase is suspended in a water phase containing a stabilizing agent. Polymerization occurs within the monomer droplets, forming a three phase system (monomer/polymer/water) when the polymer precipitates from the monomer droplet due to lack of solubility. Given the polymerization conditions are adequate, a core/shell morphology with the polymer encapsulating the hydrocarbon will be thermodynamically favored [10–14].

In this study, the monomer phase consists of acrylonitrile (AN) and methacrylonitrile (MAN) as monomers, isooctane as blowing agent, and an initiator. f_{AN}, representing the fraction of AN in the initial monomer feed, is further on used in this study when presenting and discussing the results. Each droplet in the emulsion can be kinetically seen as a micro-batch reactor if the monomers involved are water insoluble [9,15,16]. If however, as in this study, the monomers are slightly water soluble, deviations in the kinetics can be observed [17].

Even though that there are a substantial number of patents regarding thermally expandable microspheres, only a limited number of studies have been published [3,18–22]. Research on similar systems as those used in this study have been performed

* Corresponding author. Tel.: +46 8 790 82 73; fax: +46 8 790 82 83.
E-mail address: mave@polymer.kth.se (E. Malmström).

0032-3861/$ - see front matter © 2006 Elsevier Ltd. All rights reserved.
doi:10.1016/j.polymer.2006.03.013

by Kolarz et al. [23–25]. However, their primary interest have been to synthesize extensively cross-linked (up to 50 wt% divinylbenzene or 40 wt% of trimethylolpropane triacrylate) AN or MAN particles with a macroporous morphology.

Since the core/shell morphology, together with the composition of the polymer shell, is crucial for the function of the thermally expandable microspheres, it is of interest to determine the limitations of the system with respect to the particle morphology and encapsulation. The aim of this study was, therefore, to investigate, in greater detail, how the particle morphology is affected by changes in the monomer feed or the polymerization temperature.

2. Experimental

2.1. Materials

Acrylonitrile (AN), 99+%, stabilized with 35–45 ppm hydroquinone monomethyl ether, methacrylonitrile (MAN), 99%, stabilized with 50 ppm hydroquinone monomethyl ether, dilauroyl peroxide, 97%, and isopentane, 99+%, were purchased from Aldrich. Sodium hydroxide, >99.98%, and sodium 2-ethylhexyl sulfate, ~50% in water, were purchased from Fluka. Magnesium chloride, 97%, was purchased from Prelabo. All chemicals were used as received.

2.2. Suspension polymerization

Polymerizations were performed according to the general procedure presented in [4]. A dispersion of $Mg(OH)_2$ was prepared by mixing a NaOH solution (0.65 g NaOH (s) in deionized water (12.4 g)) with a $MgCl_2$ solution (2.25 g $MgCl_2 \cdot 6H_2O$ (s) in deionized water (12.4 g)) followed by vigorous stirring for at least 0.5 h. This dispersion, together with 0.3 g of a 1 wt% solution of sodium 2-ethylhexyl sulfate (aq) was mixed with an organic phase containing 9.6 g monomer (Tables 1 and 2), isopentane (2.4 g, 20 wt% of organic phase based on monomer and blowing agent as commonly used in thermally expandable microspheres [1,4,5,21,22]) and dilauroyl peroxide (0.19 g). The mixture was emulsified using an Ultra-Turrax high shear mixer for 45 s at 8000 rpm. Polymerization was conducted under agitation in a 50 ml glass pressure reactor (Tinyclave from Büchi), at 62 or 80 °C unless otherwise noted.

2.3. Work-up

Agglomerates and larger particles were removed from the dispersions using a 100 μm sieve after the polymerizations. The suspending agent was removed from the particles by acidifying to pH < 2 under stirring using sulfuric acid. After filtration were the polymeric particles finally dried for more than 48 h at ambient temperature and pressure after thorough washing with water.

2.4. Analyses

Monomer conversions were determined by gas chromatography (GC). Approximately 0.2 g of dispersion was withdrawn directly from the reactor and dissolved in 10 g of *N*,*N*-dimethyl acetamide containing THF as an internal standard. Monomer conversions were calculated from the GC results in relation to the initial monomer feeds. This method determines the total monomer conversion since monomer dissolved in the water phase will be included.

Size-exclusive chromatography (SEC) with multi-angle laser light scattering (MALLS)/refractive index (RI) detection

Table 1
Summary of polymerizations conducted at 62 °C for 23 h with various AN/MAN feed ratios

Run	f_{AN}[a]	Particle size[b] (μm)	Aggregation[c]	Conversion[d]		Molecular weight[e,f]	
				AN (%)	MAN (%)	M_w (g/mol)	PDI
1	0	21.2	3		91.6	580,000	2.5
2	0.04	19.9	3	75.5	94.9	630,000	2.5
3	0.08	16.0	3	76.8	95.5	560,000	2.9
4	0.12	15.7	3	75.3	95.4	510,000	2.7
5	0.16	16.0	2	78.2	96.4	490,000	3.2
6	0.21	19.5	2	84.3	98.1	480,000	2.9
7	0.21	21.9	2	81.8	97.6	440,000	3.0
8	0.44	11.6	1	91.4	99.8	360,000	2.9
9	0.70	14.6	1	94.3	99.9	270,000	3.0
10	0.70	14.8	1	95.1	99.9	290,000	2.9
11	0.76	14.5	1	95.5	99.9	230,000	3.2
12	0.82	15.5	1	96.4	99.9	210,000	2.6
13	0.88	13.0	1	98.3	99.9	220,000	2.3
14	0.94	12.0	1	99.1	99.8	270,000	2.5
15	1	12.3	1	99.5		340,000	4.0

[a] Fraction of acrylonitrile in the initial monomer feed.
[b] Determined by laser light scattering, presented as the volume median diameter ($d(0.5)$).
[c] Determined by visual inspection of the residual after sieving (1, none/small amount of agglomerates; 2, moderate amount; 3, major amount).
[d] Determined by GC.
[e] Determined by SEC-MALLS.
[f] Numbers have been rounded due to uncertainties in d*n*/d*c*.

Table 2
Summary of polymerizations conducted at 80 °C for 7 h with various AN/MAN feed ratios

Run	f_{AN}[a]	Particle size[b] (μm)	Aggregation[c]	Conversion[d]		Molecular weight[e,f]	
				AN (%)	MAN (%)	M_w (g/mol)	PDI
16	0	6.1	1		8.9	33,000	3.3
17	0.21	9.4	1	4.4	17.3	150,000	5.2
18	0.21	6.2	1	12.3	21.9	N.d.[g]	
19	0.21	7.2	1	9.3	25.6	N.d.[g]	
20	0.25	7.5	1	10.7	30.1	N.d.[g]	
21	0.30	6.2	2	17.6	37.1	N.d.[g]	
22	0.35	7.1	2	24.6	44.0	N.d.[g]	
23	0.39	13.8	2	34.9	62.1	N.d.[g]	
24	0.44	16.5	3	69.8	91.5	270,000	4.5
25	0.44	12.6	3	57.8	83.3	N.d.[g]	
26	0.44	12.2	3	62.9	87.7	N.d.[g]	
27	0.49	24.8	3	75.6	95.7	290,000	3.9
28	0.54	19.4	3	86.0	99.1	320,000	3.7
29	0.59	14.6	2	90.4	99.7	270,000	3.8
30	0.65	11.3	1	92.0	99.9	250,000	3.2
31	0.70	32.5	1	95.4	99.9	250,000	3.2
32	0.76	13.0	1	95.8	99.9	210,000	3.1
33	0.82	13.8	1	96.5	99.9	200,000	3.1
34	0.88	12.7	1	97.8	99.9	180,000	3.7
35	0.94	12.9	1	98.9	99.8	180,000	2.4
36	1	10.7	1	99.7		190,000	2.8

[a] Fraction of acrylonitrile in the initial monomer feed.
[b] Determined by laser light scattering, presented as the volume median diameter ($d(0.5)$).
[c] Determined by visual inspection of the residual after sieving (1, none/small amount of agglomerates; 2, moderate amount; 3, major amount).
[d] Determined by GC.
[e] Determined by SEC-MALLS.
[f] Numbers have been rounded due to uncertainties in dn/dc.
[g] Not determined.

was used to determine molecular weights. The system consisted of a Dionex P580 A, isocratic pump and a Degasys Populaire DP 2010, solvent degasser. Separation was performed by three PLGel 10 μm Mixed-B 300×7.5 mm columns (Polymer Laboratories Ltd) held at 80 °C. A Dawn EOS MALLS detector together with an Optilab DSP RI detector was used for detection. DMF with 10 mM of tetraethyl ammonium nitrate [26] was used as mobile phase at a flow rate of 0.250 ml/min. Samples were prepared by dissolving the polymer in the mobile phase by heating at 70 °C for 1 h, followed by at least 3 days of gentle shaking at ambient temperature prior to analysis. The Astra 4.90.07 software by Wyatt Technology was used to evaluate the collected data.

The refractive index increment, dn/dc, is important in the calculation of molecular weights from light scattering data. dn/dc is dependent on polymer composition, solvent and detector wave length. To the best of our knowledge, there are only a limited number of dn/dc values for PAN in DMF available in the literature [27,28]. However, these values have been determined at different wavelengths or temperatures compared to the ones used in this study. dn/dc was, therefore, determined for a selection of the polymers in this study. The polymers were dissolved in DMF, precipitated into methanol twice and dried under vacuum at 50 °C until constant weight. Polymer solutions in DMF were prepared by heating at 70 °C for 1 h and then stored at ambient temperature until measurements were conducted using an Optilab DSP RI detector set to 40 °C. DNDC for Windows 5.90.03 by Wyatt Technology was used for calculating the dn/dc values.

Thermal gravimetric analysis (TGA) was conducted on a Mettler Toledo TGA/SDTA851[e] to determine blowing agent content as well as to monitor polymer decomposition. All samples were dried prior to analysis in order to exclude as much moisture and residual monomers as possible. However, drying has to be conducted with care in order not to affect the hydrocarbon content, which is why moisture and residual monomers cannot be completely removed. Based upon experience, the amount of remaining water is approximately 0.5–1 wt% and the residual monomer content varies between 0.1 and 3 wt%. The dried samples were heated from 30 to 650 °C at 20 °C min^{-1} under N_2 atmosphere followed by isothermal analysis at 650 °C for 15 min under O_2 atmosphere.

Particle morphologies were studied using a Philips SEM XL 20 scanning electron microscope (SEM). All samples were coated with a thin layer of gold prior to analysis using a BAL-TEC SCD 005 sputter-coater (0.1–0.01 mbar, 230 s at ~35 mA). Particles were molded into an epoxy matrix at 40 °C for 3 days to enable studies of the particle cross-sections. These samples were prepared using a LKB Ultramicrotome prior to sputter-coating.

Particle size and particle size distribution were determined on a Malvern Mastersizer Hydro 2000 SM light scattering apparatus in a diluted dispersion of the particles in water. The samples were ultrasonicated for 10 min prior to analysis.

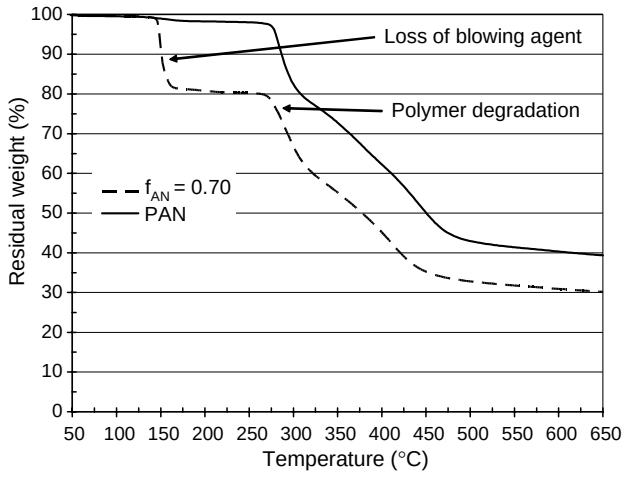

Fig. 1. Samples analyzed by TGA in order to determine volatile content. The weight loss at approximately 200 °C is considered to represent the blowing agent content.

3. Results and discussion

3.1. Particle morphology

Effective encapsulation of the blowing agent is a crucial parameter during the manufacturing of thermally expandable microspheres. Obviously, if no blowing agent is encapsulated, no expansion is possible. Thermal gravimetric analysis (TGA) was used in this study to determine the total volatile content of each sample. The weight loss below ca. 200 °C is considered to be a good estimate of the blowing agent content (Fig. 1).

From scanning electron microscopy (SEM) images, it is evident that the particle morphology is affected, both by the monomer feed composition and the polymerization temperature (Figs. 2–4). Depending on the parameters of the polymerization, various morphologies are obtained, ranging from solid particles (Fig. 2(A)), particles with core/shell structure (Fig. 2(B)–(D)) to particles built up from agglomerated primary particles (Fig. 2(E)).

There are several factors influencing the particle morphology during suspension polymerization. The final particle morphology is dependent on the extent to which the polymer

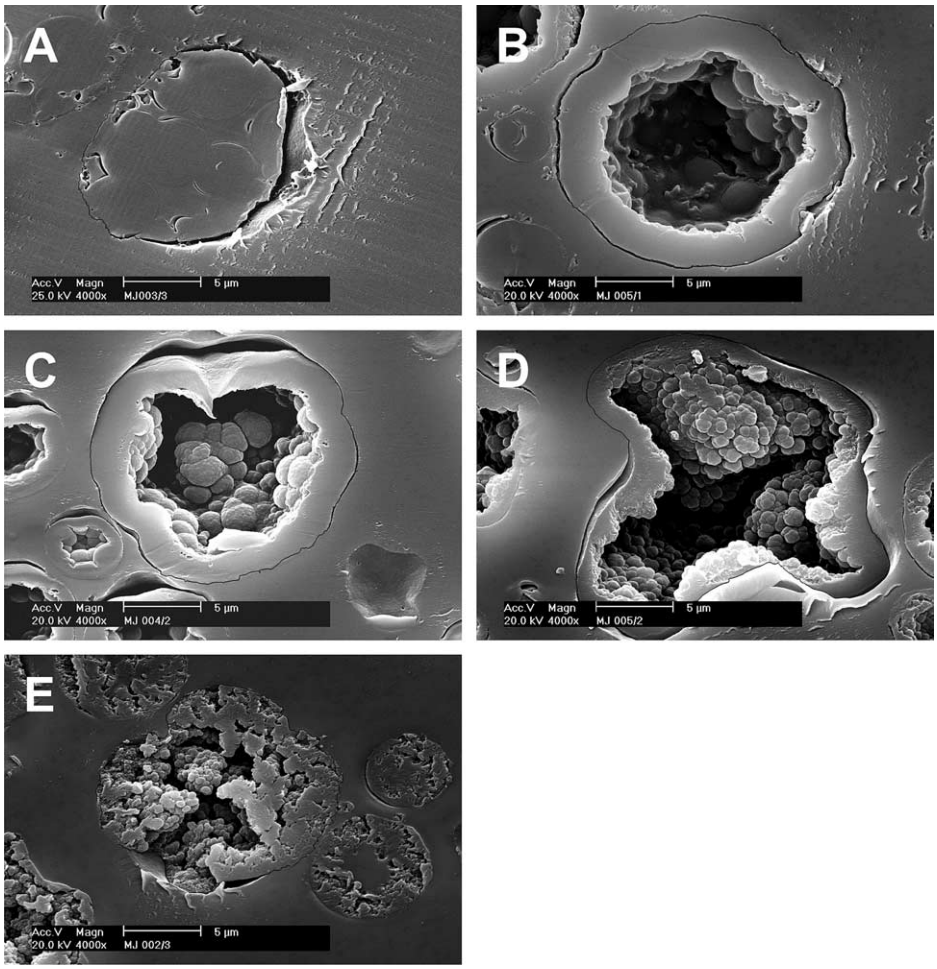

Fig. 2. SEM images of morphologies in cross-sections of particles (polymerized at 62 °C) moulded into an epoxy matrix. (A) $f_{AN}=0$ (B) $f_{AN}=0.21$ (C) $f_{AN}=0.44$ (D) $f_{AN}=0.70$ (E) $f_{AN}=1$. In these images, the particle/matrix interface has been highlighted by a thin black line to increase view ability using Adobe Photoshop Elements.

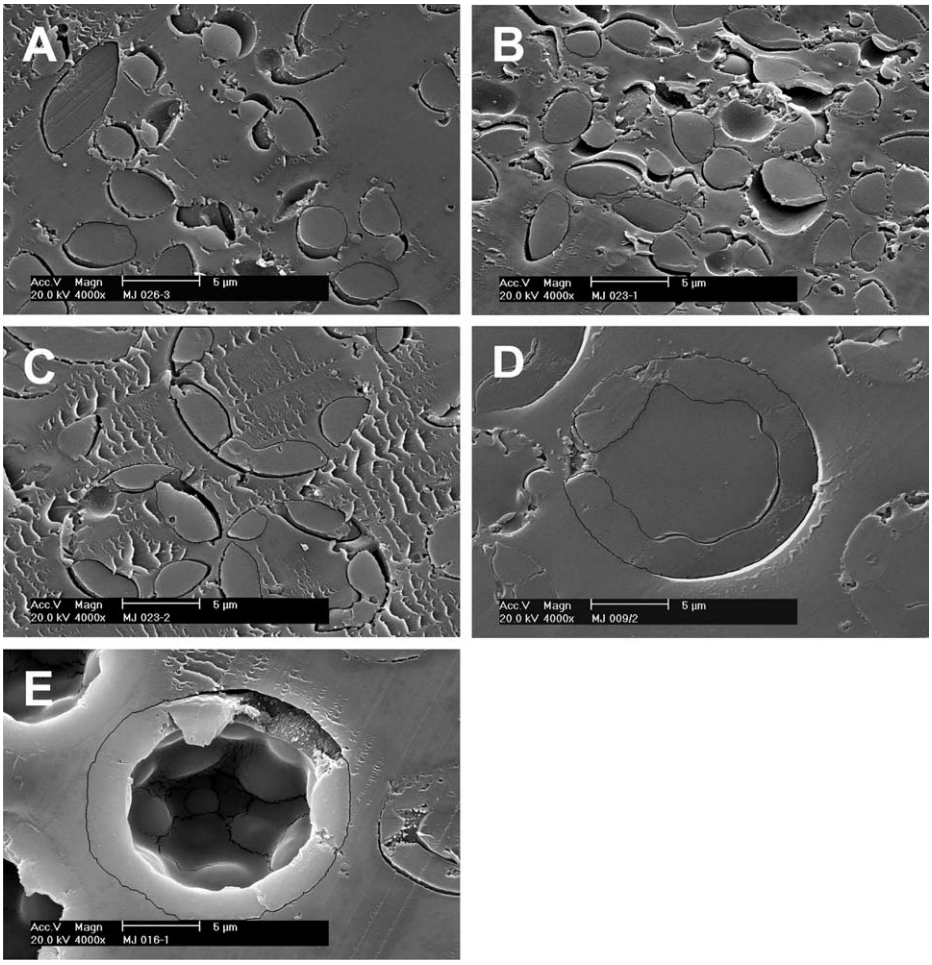

Fig. 3. SEM images of morphologies in cross-sections of particles (polymerized at 80 °C) moulded into an epoxy matrix. (A) $f_{AN}=0.30$ (B) $f_{AN}=0.35$ (C) $f_{AN}=0.39$ (D) $f_{AN}=0.44$ (E) $f_{AN}=0.49$. The inner cavity of the particles in C and D is filled by the epoxy matrix in which the particles are moulded. In these images, the particle/matrix interface has been highlighted by a thin black line to increase view ability using Adobe Photoshop Elements.

dissolves, swells or precipitates in the organic phase. Smooth clear beads are generally formed in suspension copolymerization when both homopolymers are soluble in their respective monomer (e.g. styrene–methyl methacrylate). Opaque, irregular beads are formed when both polymers precipitate from their monomer (e.g. vinyl chloride–acrylonitrile) [7–9,29,30].

According to the literature [31,32], the situation is more complicated when methacrylonitrile is suspension polymerized as the solubility of PMAN is dependent on both molecular weight as well as reaction temperature. It is suggested that a two phase system forms within the organic phase in which the monomer phase is saturated with polymer while the composition of the other phase is dependent on the polymerization parameters.

The particle morphology is also dependent on the surface tensions of the various components (i.e. polymer, monomer, continuous phase) during polymerization. A desire to minimize the interfacial energy is the driving force determining whether or not core/shell particles, hemispheres, individual particles or other possible morphologies will form (Fig. 5). This was first investigated by Torza and Mason [10], who studied a system of two immiscible oils suspended in water. They found that the particle morphology can be predicted from the surface tensions of the components. Later Sundberg et al. examined water/polymer/oil systems [11], water/polymer/polymer systems [12] and found that these systems act in a similar way with respect to the particle morphology. According to them, a core/shell morphology will be thermodynamically favoured during polymerization if

$$\gamma_{wo} > (\gamma_{wp} + \gamma_{op})$$

in which γ_{wo} is the interfacial tension of the water and the oil interphase, γ_{wp} is the interfacial tension of the water/polymer interface and γ_{op} is the interfacial tension of the oil/polymer interface. The described water/polymer/oil system will correspond to the water/polymer/(monomer and blowing agent) system in our study.

3.2. Polymerizations at 62 °C

In this study, the polymerization temperature is an important parameter as it determines the rate of radical formation. The 10 h half-life temperature of dilauroyl peroxide is 61 °C [33]. A polymerization temperature of 62 °C, therefore, yields radicals

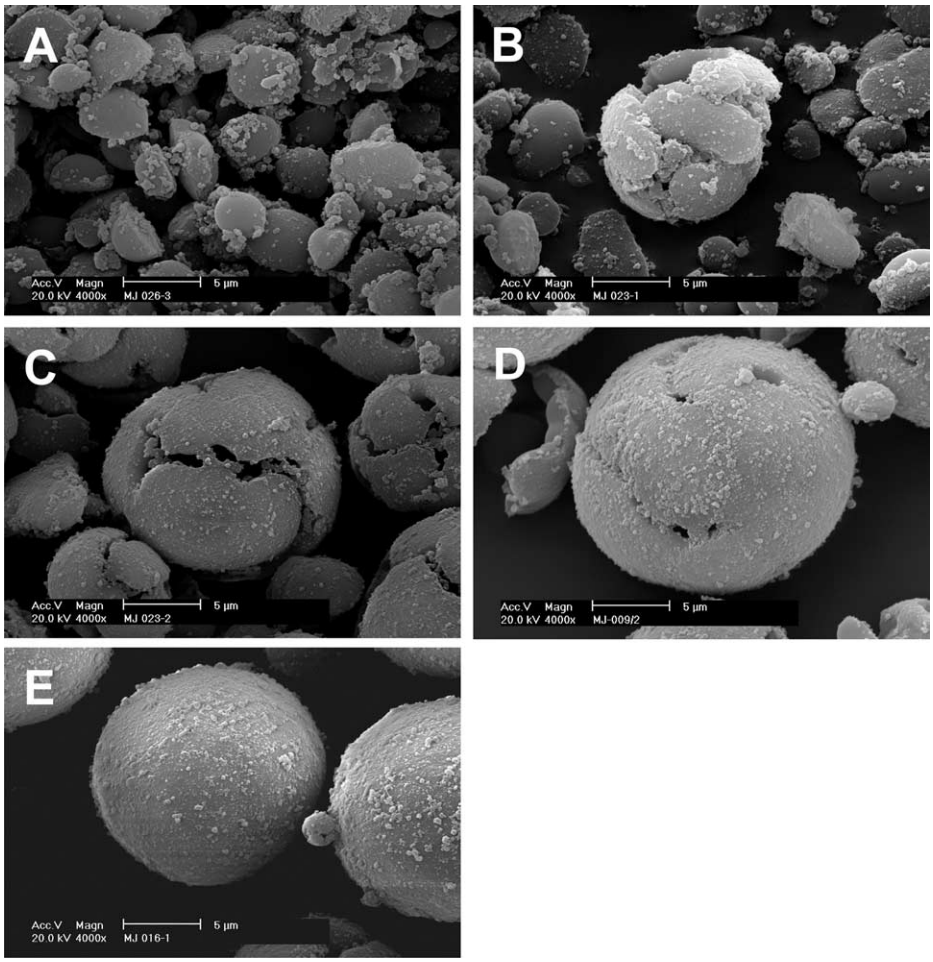

Fig. 4. SEM images of particle morphology after polymerization at 80 °C. (A) $f_{AN}=0.30$ (B) $f_{AN}=0.35$ (C) $f_{AN}=0.39$ (D) $f_{AN}=0.44$ (E) $f_{AN}=0.49$.

at a relatively moderate rate as compared to at 80 °C since the 1 h half-life temperature of this initiator is 79 °C. Polymerizations at 62 °C were conducted for 23 h (30 min of heating from 25 °C not included). The results from the polymerizations at 62 °C can be found in Table 1.

The mean particle sizes, measured with light scattering, range from approximately 12–22 µm. The differences in particle size are primarily caused by variations in the emulsion stability during polymerization. When polymerizing at 62 °C, it was observed that there is a tendency for an increasing amount of agglomerates with decreasing f_{AN} (Table 1). These agglomerates were removed prior to analysis. We did not make any attempts to optimize the stabilisation system in order to avoid these agglomerates since we wanted to keep all parameters constant except for the monomer feed composition.

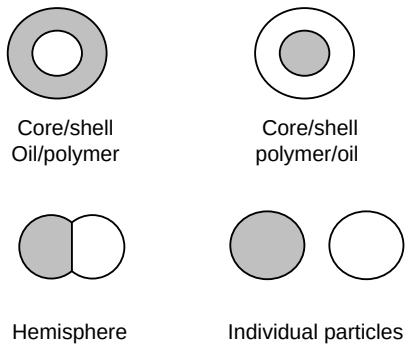

Fig. 5. Examples of particle morphologies that may form depending on the polymerization parameters with grey areas representing polymer.

The overall monomer conversion was above 90% regardless of the monomer feed composition (Fig. 6). As can be seen in Fig. 6, the monomer conversion increases with increasing f_{AN}. Actually the homopolymerization of AN ($f_{AN}=1$) reaches 99.5% conversion, which is surprisingly high considering that Lu et al. [34] has shown that the conversion of AN in suspension homopolymerization is limited due to the water solubility of AN (8.4 wt% at 50 °C). Monomer dissolved in the water phase limits the conversion unless there is a competing polymerization in the water phase, or there is a back transfer of monomer to the non-aqueous phase. It has been shown that dilauroyl peroxide gives negligible water phase polymerization when used as a free-radical initiator in suspension polymerization [35,36]. As the polymerization proceeds, due to the inert blowing agent, there is a drift in the composition of the monomer droplet, thus creating a driving force for re-establishing the equilibrium of AN between the phases. This diffusion of monomer from the water phase to the monomer droplet occur even though the polymer shell has formed early in the process.

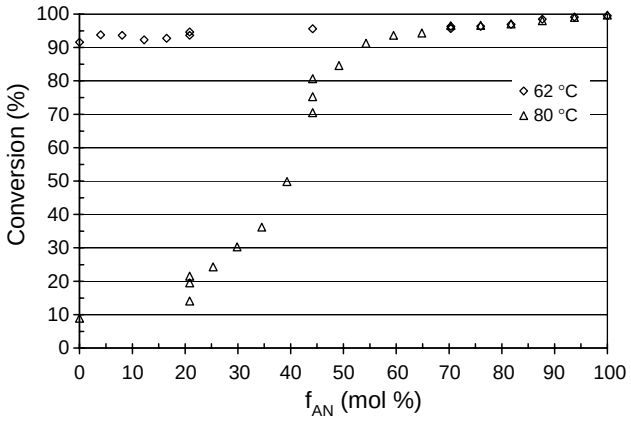

Fig. 6. Total monomer conversion as determined by GC after polymerization with various monomer feeds and temperatures.

SEC-MALLS data show that polymerization at 62 °C gives high molecular weights (Fig. 7). There is a nearly linear decrease in molecular weight from approximately 600,000 g/mol for PMAN with increasing f_{AN}, to a lowest level of 210,000 g/mol at $f_{AN}=0.82$.

Poor dissolution of the polymer samples in the mobile phase caused some problems in the molecular weight determinations. The increase in molecular weights at $f_{AN}>0.85$ are caused by agglomerates due to poor solubility. This was also apparent in the determination of the d*n*/d*c* values used in the molecular weight calculations. The uncertainties of the molecular weights presented in Table 1 are, therefore, considered to be significant. The molecular weight ratios of polymers of similar composition (equal f_{AN}, polymerized at either 62 or 80 °C) are, however, independent of the d*n*/d*c* values.

Clearly the polymerization temperature as well as the composition of the monomer feed is important for encapsulation of the blowing agent (Fig. 8). When polymerizing at 62 °C, the blowing agent is sufficiently (volatile content >15 wt%) encapsulated for $f_{AN}=0.15$–0.95.

The particle morphologies were examined by SEM to prove the encapsulation results determined by TGA. It is evident that the particle morphology is dependent on the monomer feed. The SEM images reveal that the PMAN particles (Fig. 2(A)) are solid, thus explaining the lack of blowing agent (Fig. 8). As f_{AN} increases, there is a transition from solid particles into a core/shell morphology. $f_{AN}=0.21$ (Fig. 2(B)) gives core/shell particles with the polymer encapsulating the blowing agent. This transition occurs as early as at $f_{AN}=0.04$; however, it is then a mixture of mainly solid particles with some core/shell particles. The core/shell particle fraction increases with increasing f_{AN} up to approximately $f_{AN}=0.12$, when the vast majority of the particles have the core/shell morphology. The texture of the inner surface of the core/shell particles is affected by increases in f_{AN} as well. It gets rougher as revealed by the SEM images of particles in which $f_{AN}=0.21$–0.70 (Fig. 2(B)–(D)). These particles all sufficiently encapsulate the blowing agent (Fig. 8). The particles, in which $f_{AN}>0.90$, does not have the core/shell morphology, they are instead made up of agglomerated primary particles (Fig. 2(E)). The particles, in which $f_{AN}=0.95$, contain blowing agent trapped inside. Even though the PAN particle has a smooth outer shell, the barrier properties of this shell are not enough to retain the blowing agent (Fig. 8).

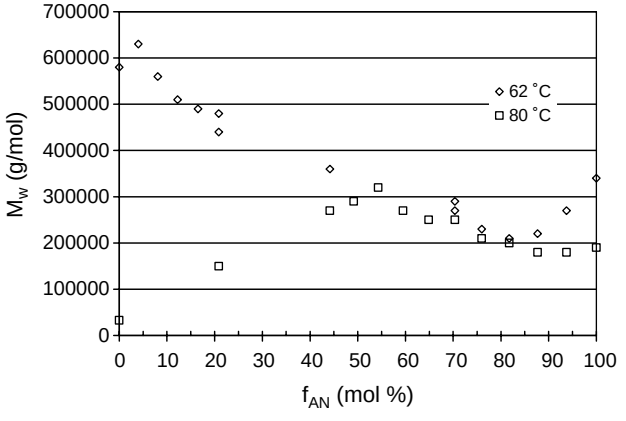

Fig. 7. Molecular weights as determined by SEC-MALLS after polymerization with various monomer feeds and temperatures.

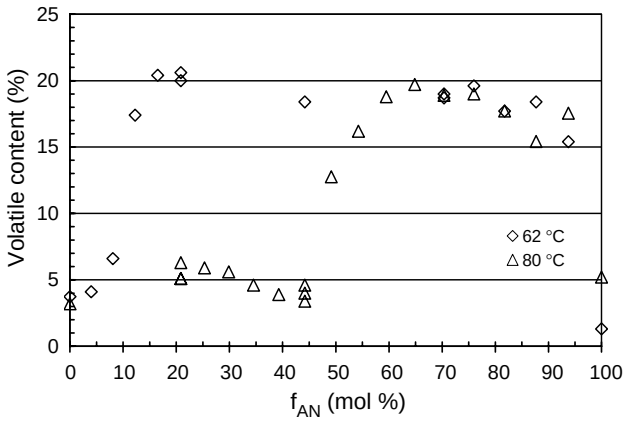

Fig. 8. Volatile content as determined by TGA, representing the weight loss at 200 °C. The volatile content includes blowing agent, residual monomer and moisture.

3.3. Polymerizations at 80 °C

The 1 h half-life temperature of dilauroyl peroxide is 79 °C [33]. Polymerizations at 80 °C were, therefore, conducted for 7 h (1 h of heating from 25 °C up to 80 °C not included) leaving virtually no remaining initiator. The results from the polymerizations at 80 °C can be found in Table 2.

The particle size and its distribution, as well as the formation of agglomerates show a different pattern as compared with the polymerizations at 62 °C (Table 2). At $f_{AN}<0.25$, the particles are smaller than 10 μm in size with no formation of agglomerates. However, at intermediate f_{AN} there is a tendency for larger particles and more agglomerates, while above $f_{AN}=0.65$ the particle size is well controlled with only a limited formation of agglomerates.

When the polymerization is carried out at 80 °C, there is a large dependency of f_{AN} on the monomer conversion. For instance, the homopolymerization of MAN ($f_{AN}=0$) only

reaches 10% conversion. However, as f_{AN} increases, there is a dramatic increase in conversions reaching above 90% at $f_{AN}=0.54$ (Fig. 6).

The encapsulation process is also dependent on the polymerization temperature. Satisfactory encapsulation is only accomplished at 80 °C when $f_{AN}=0.5$–0.95 (Fig. 8). The SEM images of the particle cross-sections give further proof of this. Until f_{AN} reaches 0.35, solid particles resembling of the PMAN particles at 62 °C are formed (Figs. 3(A) and 4(A)). Unlike the morphology transition at 62 °C, in which there is a mixture of solid and core/shell particles in the morphology transition, there is another mechanism at 80 °C in the interval of $f_{AN}=0.35$–0.49 (Figs. 3 and 4).

In this transition, the polymer shell of the core/shell particles is formed as the solid particles form clusters (Fig. 4(B)–(E)). This cluster formation begin at approximately $f_{AN}=0.35$ (Fig. 4(B)). From the SEM image of the particle cross-section, it is evident that the core/shell morphology is beginning to form as f_{AN} increase to 0.39 (Fig. 3(C)). The average particle size further indicates this cluster formation as there is a leap in particle size from $f_{AN}=0.35$ to $f_{AN}=0.39$ (Table 2). It is, however, clear that the polymer shell is not tight and that no blowing agent can be retained (Figs. 4(C) and 8). At $f_{AN}=0.49$, there is sufficient encapsulation to retain the blowing agent (Figs. 3(E), 4(E) and 8). However, it is not until $f_{AN}=0.60$ that there is complete encapsulation (Fig. 8).

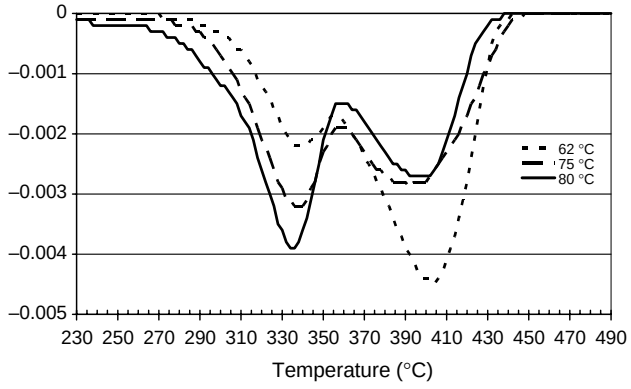

Fig. 9. Relative rate of PMAN depolymerization for polymers polymerized at 62, 75 and 80 °C. The curves are derived from the TGA analysis of the respective samples in the region of the polymer breakdown.

The molecular weight of the polymers polymerized at 80 °C show a different pattern than was seen for those polymerized at 62 °C. Instead of a molecular weight of approximately 600,000 g/mol for PMAN with a nearly linear decrease as f_{AN} increase, the molecular weight for PMAN at 80 °C is only 33,000 g/mol. The molecular weight then increases with increasing f_{AN} until $f_{AN}=0.55$ (Fig. 7). The molecular weights above $f_{AN}=0.55$ are independent of the polymerization temperature and those reached at 80 °C coincides with those reached at 62 °C.

The results indicate that at 62 °C, it is the solubility of the polymer that is the determining parameter irrespective of the composition, whereas at 80 °C, the molecular weights are kinetically determined at $f_{AN}<0.55$ with an increasing rate of termination with decreasing f_{AN}, while at $f_{AN}>0.55$, the molecular weights are thermodynamically determined in a similar way as at 62 °C. Low conversions in the experiments with kinetically determined molecular weights further confirm this increase in the termination rate (Fig. 6).

It is interesting to note that the molecular weight of PMAN polymerized at 62 °C is approximately 20 times higher than the corresponding polymer polymerized at 80 °C. This may partly be explained by differences in the termination mechanism [37]. At 62 °C, termination occurs mainly by the coupling mechanism. At 80 °C, there is an increase in termination by the disproportionation mechanism, thus decreasing the molecular weight. This change in termination mechanism is verified in a study of the thermal decomposition of PMAN samples polymerized at various temperatures (62, 75 and 80 °C), in which the polymerization at 75 °C was conducted for further confirmation. Thermal decomposition of PMAN occurs in two steps [38], initially at chain ends terminated by disproportionation and, therefore, containing unsaturations. At higher temperatures, random chain scission increases the number of sites for depolymerization. The relative rate of depolymerization as measured by TGA (Fig. 9) clearly shows that the depolymerization by the initial mechanism, i.e. at chain ends from disproportionation, increases with increasing polymerization temperature.

Table 3
Summary of polymerizations conducted for various times at 62 °C with $f_{AN}=0.70$

Run	Polymerization time (h)	Particle size[a] (μm)	Aggregation[b]	Conversion[c]		Molecular weight[d,e]	
				AN (%)	MAN (%)	M_w (g/mol)	PDI
37	1	14.1	1	9.8	19.7	280,000	1.9
38	2	11.6	1	20.3	36.3	290,000	1.9
39	3	10.9	1	29.8	51.0	280,000	2.0
40	5	10.8	1	47.1	72.7	260,000	2.0
41	8	15.6	1	74.6	95.1	260,000	2.2
42	23	14.2	1	95.3	99.9	250,000	2.7

[a] Determined by laser light scattering, presented as the volume median diameter ($d(0.5)$).
[b] Determined by visual inspection of the residual after sieving (1, none/small amount of agglomerates; 2, moderate amount; 3, major amount).
[c] Determined by GC.
[d] Determined by SEC-MALLS.
[e] Numbers have been rounded due to uncertainties in dn/dc.

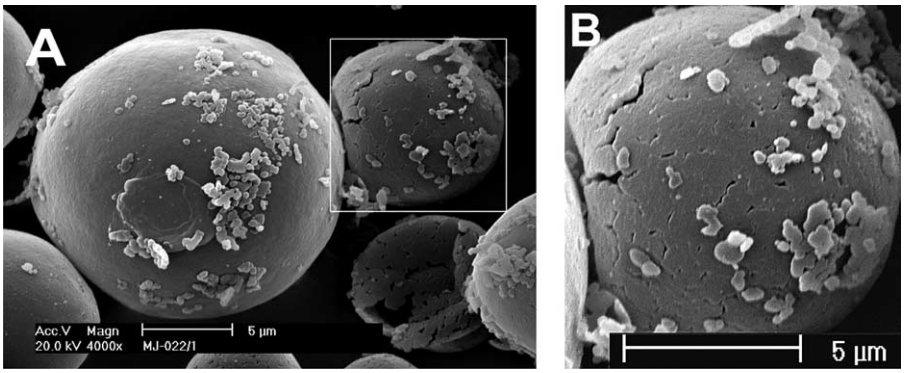

Fig. 10. SEM images of the polymer shell formation. (A) Particles after 1 h of polymerization at 62 °C ($f_{AN}=0.70$). (B) Enlargement of part of A.

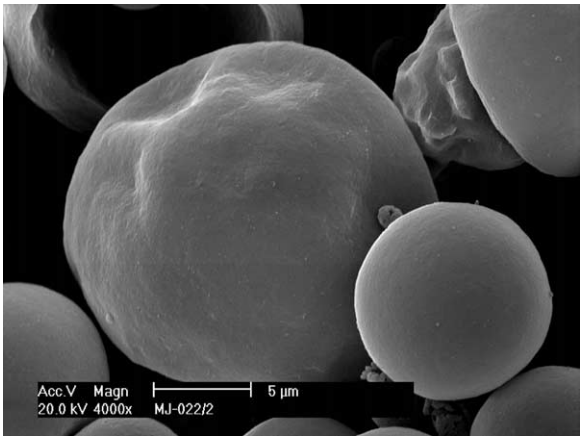

Fig. 11. SEM image of the particle polymer shell after 2 h of polymerization at 62 °C ($f_{AN}=0.70$).

3.4. Polymer shell formation at 62 °C

In order to further elucidate the shell formation, its correlation to polymerization time and monomer conversion was studied. The results of this study can be found in Table 3. A monomer composition in which $f_{AN}=0.70$ was chosen as polymerization at either 62 or 80 °C gave a core/shell morphology. Samples were collected during the polymerization that was conducted at 62 °C. The monomer conversion was determined in these samples and the polymer particles were examined by SEM (Figs. 10–12). The skeleton of the polymer shell has already been formed by primary particles after 1 h, even though the overall monomer conversion is only 12% (Fig. 10). These primary particles precipitate from the monomer phase and arrange at the interphase of the monomer droplet and the water phase. After 2 h of polymerization, when the overall conversion is ca. 24%, a thin smooth particle shell has formed (Figs. 11 and 12(A)). As the polymerization proceeds, the shell gets thicker with a rougher inner surface (Fig. 12(B)–(D)).

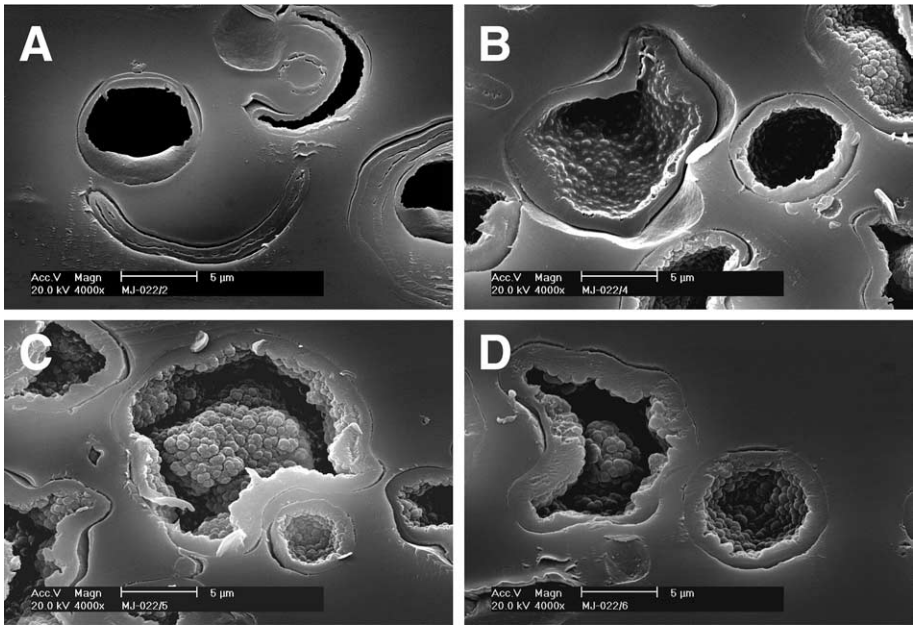

Fig. 12. SEM images of particle cross-sections of particles collected during polymerization at 62 °C ($f_{AN}=0.70$). (A) After 2 h (B) 5 h (C) 8 h (D) 23 h.

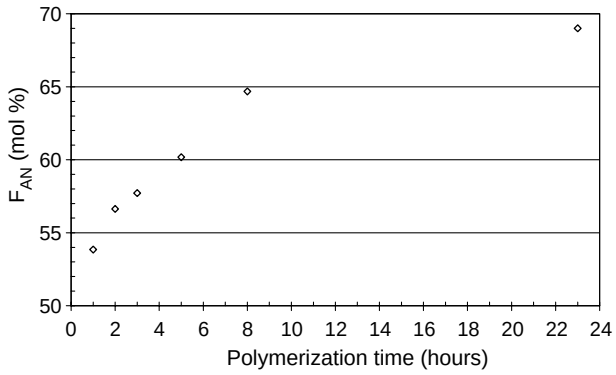

Fig. 13. Drift in the average copolymer composition during polymerization at 62 °C (f_{AN} = 0.70). The monomer conversions determined by GC were used in the calculation.

During polymerization, there is a drift in the polymer composition. Polymer formed early in the polymerization is rich in MAN as it has the highest reactivity in the copolymerization with AN (r_1 = 0.43, r_2 = 1.67) [39], while polymer formed late is rich in AN. This drift in polymer composition is illustrated in Fig. 13, in which the average polymer AN ratios (F_{AN}) were calculated from the monomer conversions determined by GC.

The results of this study indicate that there are different mechanisms involved in the shell formation when polymerizing at 62 °C vs. at 80 °C. At 62 °C, the mixture of solid and core/shell particles indicate that the composition of the copolymer formed initially is decisive for the final morphology of the particle. If the polymer mainly consists of MAN, solid particles form while initial polymer with a relatively high AN content will tend to form core/shell particles. At 80 °C, the SEM images indicate that there is another mechanism involved. Small solid particles form clusters that finally give core/shell particles. However, we do not know how this mechanism works. At the opposite end of the monomer feed composition, i.e. the PAN particles that do not have the core/shell morphology, we propose that the morphology is kinetically determined. A large number of primary particles form early in the polymerization and cluster, reducing the mobility of the particles why no core/shell morphology may form.

4. Conclusions

The monomer feed composition, as well as the polymerization temperature, are important parameters in determining the particle morphology of suspension polymerized co-acrylonitrile polymer particles. A core/shell morphology is attained for f_{AN} = 0.15–0.90 when polymerizing at 62 °C. At 80 °C, the core/shell morphology is more dependent on the monomer feed composition. It was found that f_{AN} = 0.5–0.85 results in the desired core/shell morphology. The particle shell is formed by coalescence of primary particles into a tight shell that increases in thickness as the polymerization proceeds.

Acknowledgements

The Swedish Research Council and Akzo Nobel are gratefully acknowledged for their financial support. Taina Tollgren and Elin Andersson are acknowledged for the SEM images, while Analyscentrum at Casco Adhesives AB is acknowledged for their assistance with the SEC-MALLS measurements.

References

[1] Morehouse DSJ, Tetreault RJ. US 3,615,972; 1964.
[2] Elfving K. Blowing agents and foaming processes. Munich, Germany: Rapra Technology Ltd; 2003. p. 17–24.
[3] Ahmad M. J Vinyl Addit Technol 2001;7:156–61.
[4] Lundqvist J. EP 0 486 080 B1; 1992.
[5] Yokomizo T, Tanaka K, Niinuma K. JP 9019635; 1997.
[6] Soane DS, Houston MR. US 6,617,364 B2; 2003.
[7] Dowding PJ, Vincent B. Colloids Surf, A 2000;161:259–69.
[8] Munzer M, Trommsdorff E. Polymerizations in suspension. In: Schildknecht CE, Skeists I, editors. High polymers, vol. 29. New York: Wiley; 1977. p. 106–42.
[9] Yuan HG, Kalfas G, Ray WH. J Macromol Sci, Rev Macromol Chem Phys 1991;C31:215–99.
[10] Torza S, Mason SG. J Colloid Interface Sci 1970;33:67–83.
[11] Berg J, Sundberg D, Kronberg B. J Microencapsulation 1989;6:327–37.
[12] Sundberg DC, Casassa AP, Pantazopoulos J, Muscato MR, Kronberg B, Berg J. J Appl Polym Sci 1990;41:1425–42.
[13] Ma G, Li J. Chem Eng Sci 2004;59:1711–21.
[14] Ma G-H, Omi S. Macromol Symp 2002;179:223–40.
[15] Kalfas G, Ray WH. Ind Eng Chem Res 1993;32:1822–30.
[16] Kalfas G, Yuan H, Ray WH. Ind Eng Chem Res 1993;32:1831–8.
[17] Zhang SX, Ray WH. Ind Eng Chem Res 1997;36:1310–21.
[18] Nishiyama Y, Uto N, Sato C, Sakurai H. Int J Adhes Adhes 2003;23:377–82.
[19] Huang Y, Dimonie VL, Klein A. Polym Mater Sci Eng 2004;90:742.
[20] Huang Y, Klein A, Dimonie VL. Polym Mater Sci Eng 2003;89:769.
[21] Kawaguchi Y, Oishi T. J Appl Polym Sci 2004;93:505–12.
[22] Kawaguchi Y, Itamura Y, Onimura K, Oishi T. J Appl Polym Sci 2005;96:1306–12.
[23] Kolarz BN, Wojaczynska M, Trochimczuk AW. Makromol Chem 1993;194:1299–306.
[24] Kolarz BN, Trochimczuk AW, Wojaczynska M, Drewniak M. Angew Makromol Chem 1994;217:19–29.
[25] Kolarz BN, Wojaczynska M, Bryjak J, Pawlow B. React Polym 1994;23:123–30.
[26] Mourey TH, Bryan TG. J Chromatogr A 2002;964:169–78.
[27] http://www.changkyung.co.kr/nft/scanref/body_pan_in_dmf.htm; 2005.
[28] Brandrup J, Immergut EH. Polymer handbook. 4th ed. New York: Wiley; 1999 p. VII-588.
[29] Arshady R. Colloid Polym Sci 1992;270:717–32.
[30] Grulke EA. Suspension polymerization. Encycl Polym Sci Eng, vol. 16. New York: Wiley-Interscience; 1989 p. 443–73.
[31] Ball LE, Curatolo BS. Methacrylonitrile polymers. Encycl Polym Sci Eng, vol. 9. New York: Wiley-Interscience; 1987 p. 669–706.
[32] Grassie N, Vance E. Trans Faraday Soc 1956;52:727–33.
[33] Product Data sheet from www.akzonobel-polymerchemicals.com; ROW HP 66000.12/July; 2004.
[34] Lu Q, Weng Z, Zhou S, Huang Z, Pan Z. Eur Polym J 2002;38:1337–42.
[35] Cunningham MF. Polym React Eng 1999;7:231–57.
[36] Zhou S-X, Weng Z-X, Huang Z-M, Pan Z-R. J Appl Polym Sci 2001;79:1431–8.
[37] Bamford CH, Eastmond GC, Whittle D. Polymer 1969;10:771–83.
[38] McNeill IC, Mahmood T. Polym Degrad Stab 1994;45:285–91.
[39] Brandrup J, Immergut EH. Polymer handbook. 4th ed. New York: Wiley; 1999 p. II-290.